JOURNAL OF MATERIALS SCIENCE 35 (2000) 2683–2688

Synthesis by a soft chemistry route and characterization of $Li_xNi_{1-x}O$ ($0 < x < 0.5$) compounds: Behavior in molten carbonates

C. BELHOMME, M. CASSIR*, J. DEVYNCK
Laboratoire d'Electrochimie et de Chimie Analytique (UMR 7575), Ecole Nationale Supérieure de Chimie de Paris, 11 rue Pierre et Marie Curie 75231 Paris Cedex 05, France
E-mail: cassir@ext.jussieu.fr

G. GREGOIRE
Laboratoire de Chimie Appliquée de l'Etat Solide (UMR 7574), Ecole Nationale Supérieure de Chimie de Paris, 11 rue Pierre et Marie Curie 75231 Paris Cedex 05, France

$Li_xNi_{1-x}O$ powders and $Li_xNi_{1-x}O$/Au with $0 < x < 0.5$ are synthesized by a soft chemistry route. Analysis of $Li_xNi_{1-x}O$ by XRD shows an evolution from NiO ($0 < x < 0.3$) to $LiNiO_2$ ($0.3 < x < 0.5$) structures. The stability of $Li_xNi_{1-x}O$/Au ($0 < x < 0.5$) compounds synthesized by soft chemistry is studied in molten $(Li_{0.52}Na_{0.48})_2CO_3$ eutectic at 650°C, under the cathode atmosphere used in molten carbonate fuel cells (air/CO_2: 70/30). After a 48 h immersion, analysis by XRD of the lithiated nickel oxide shows that lithium ions diffuse from the oxide to the bulk of the melt. The major oxide detected at the surface of the sample has a composition very close to that of NiO formed *in situ* at the surface of a nickel foil. Hence, highly lithiated nickel oxides are not stable in the melt. $Li_xNi_{1-x}O$ is rapidly transformed confirming the very high stability of Ni(II) in the working conditions.

1. Introduction

Molten Carbonate Fuel Cell (MCFC) is regarded as a clean and efficient power source device for the future. The stage of prototypes has nowadays reached a promising stage: after the recent experience of a 2 MW stack in Santa Clara, a 1 MW-class MCFC installation will soon be starting in Japan [1, 2]. The features of a 10-kW MCFC stack has been recently studied [3]. Nevertheless, MCFC is not yet commercially available because of its limited lifetime. Indeed, the corrosion, the dissolution of the cathode and the current collectors are crucial problems [3].

This paper will be focussed on the cathode. Different metals, such as nickel, cobalt or iron and several oxides like NiO and $LiCoO_2$ have been studied as cathode materials for MCFC by many researchers [4–9]. Currently, the cathode is constituted of lithiated nickel oxide formed *in situ* in molten Li_2CO_3/K_2CO_3 or Li_2CO_3/Na_2CO_3. Initially, the cathode is in metallic nickel; but rapidly, as nickel is exposed to molten carbonates under an atmosphere composed of O_2/CO_2, it is oxidized. On account of its temperature of formation, the nickel oxide layer is not stoichiometric: positive holes are present and the formula is $Ni_{1-z}O$. Moreover, alkali species, lithium in particular, provided by the electrolyte, can be incorporated in its structure, which enhances its conductivity. Indeed, the conductivity of NiO is strongly associated with the concentration of crystal defects [10]. The amount of lithium is estimated at 1 and 4 at. % [11] and the presence of sodium has been detected by XPS [12]. The formula of the stable compound of nickel in the Li_2CO_3/Na_2CO_3 (52-48 mol %) eutectic seems to be $Li_xNa_yNi_{1-(x+y)}O$, with x and y at about one per cent. Therefore, the role played by alkali and lithium species has drawn the attention of different authors [13, 14]. In effect, the influence of the lithium amount is crucial for the increase of the cathode conductivity and its electrochemical behavior. A thorough study of lithiated nickel oxide in molten carbonate is of great interest since there are no general data on their thermodynamic stability and in particular $LiNiO_2$.

$Li_xNi_{1-x}O$ ($0 < x < 0.5$) materials have often been studied for their potential applications as cathodic materials for lithium ion batteries and as cathode materials for MCFC. In this last case, $Li_xNi_{1-x}O$ materials have already been prepared using solid-state reactions by several research teams. Some of them prepared $Li_xNi_{1-x}O$ by reacting nickel hydroxide and lithium hydroxide at 700°C for 2 hours in air [15]. In a recent article, Antolini realized a liquid phase sintering of $Li_xNi_{1-x}O$ solid solutions for $x = 0.3$ and $x = 0.44$ by the reaction of nickel powder with lithium carbonate at 750°C for different heating durations [16].

* Author to whom all correspondence should be addressed.

In this paper, a soft chemistry route is developed in order to synthesize $Li_xNi_{1-x}O$ ($0 < x < 0.5$) compounds, with structures between NiO and $LiNiO_2$. This process has already been used to prepare $LiNiO_2$ as cathodic material for lithium ion batteries [17]. Due to the high reactivity of the reagents and the media, synthesis preparation is shorter than solid-state reaction processes. The principal aim of these syntheses is to evaluate the stability of the prepared compounds in the carbonate melt. The lithiated samples were analyzed by X-ray diffraction (XRD) before and after their exposure to the melt in order to follow the influence of the electrolyte on the lithium amount in the NiO lattice. Two types of $Li_xNi_{1-x}O$ samples were studied: powders and thin films coated on gold by a dip coating technique. The main interest of the coating on gold is specifically to simulate the properties of the nickel oxide layer formed *in situ* on nickel without taking into account the corrosion of the support metal itself. The structure of $Li_xNi_{1-x}O$ ($0 < x < 0.5$) compounds are determined by Rietveld refinement.

2. Experimental

2.1. Synthesis

Lithium hydroxide (LiOH, H_2O) and nickel nitrate ($Ni(NO_3)_2$, $6H_2O$), Normapur reagents of analytical purity (>98%) were used to synthesize $Li_xNi_{1-x}O$ with $0 < x < 0.5$. The synthesis route was as follows: a solution of $(1-x)$ mol of $Ni(NO_3)_2$ was prepared in water and added to a solution of x mol of LiOH in NH_4OH. Gelatinous green precipitates of $Ni(OH)_2$ were formed. Remaining water and ammonia were partially removed by rotating evaporator at 80°C. At this stage of the experiment, two kinds of sample can be prepared. Either the gelatinous precipitate was directly treated thermally, obtaining a powder, or it was coated on a gold flag before thermal treatment in order to realize a thin film. Both samples were then calcined in a tubular furnace with a heating rate of 10°C/min up to 700°C; this temperature was maintained constant during 5 hours, under an oxygen flow to favor the formation of nickel (III). After thermal treatment the samples were quenched at room temperature.

The principal advantage of $Li_xNi_{1-x}O$/Au samples was the possibility to compare directly the behavior of these lithiated nickel oxide compounds with NiO formed *in situ* from nickel. The main drawback of this deposition was the more complicated refinement of the structure because of the introduction of a second phase.

Lithium and sodium carbonates, mixed in a ratio of 52-48 mol %, were Merck reagents of analytical purity (>98%). The cathodic atmosphere was composed of air/CO_2 in a ratio of 70-30%. Carbon dioxide of high purity grade (N45) was dried over silica gel. The cell was a compact single-compartment crucible of dimension $70 * 60$ mm^2 hermetically sealed by a stainless steel cover with a Viton O-ring. $Li_xNi_{1-x}O$ ($0 < x < 0.5$) samples were coated on gold foils of $10 * 10$ mm^2 (Engelhard CLAL). The thickness of the powder layer was about 10 μm. The temperature was controlled at 650°C with a West 6100 Gulton regulator and a calibrated chromel-alumel thermocouple.

The electrode was quenched out of the cell, its surface being recovered by a thin film of carbonate. Afterwards, this carbonate layer was rapidly washed with a stream of iced water, avoiding a large contact between water and the lithiated surface.

2.2. X-ray powder diffraction analysis

The samples of $Li_xNi_{1-x}O$/Au were analyzed before and after the exposure to the Li_2CO_3-Na_2CO_3 (52-48 mol %) eutectic, at 650°C under an atmosphere of air/CO_2 (70/30%), by XRD with a Siemens D5000 diffractometer using Co K_α ($\lambda = 1.7889$ Å) and a back graphite monochromator. The diffraction pattern was scanned by steps of 0.01° (2θ) with a fixed counting time (6 s) between $20 < 2\theta < 100°$. The structure of $Li_xNi_{1-x}O$ powder and $Li_xNi_{1-x}O$/Au were refined by the means of the Rietveld method. The lattice parameters and the real lithium ratio present in the compound were determined. The refinement was performed by using the Fullprof program and peak shapes were described by pseudo Voigt-functions [18]. The Rietveld procedure requires a structural model to refine. For $0 < x < 0.3$, the $Li_xNi_{1-x}O$ structure refinement was started with the model of NiO [19]. For $0.3 < x < 0.5$, the $Li_xNi_{1-x}O$ structure refinement was started with the model of $LiNiO_2$ [20].

For $Li_xNi_{1-x}O$/Au compounds, gold was considered as a second phase. Gold is crystallized in a fm3m space group; its lattice parameter is 4.0786 Å. The structure refinement was started with a model described in the literature [21, 22].

3. Crystallographic data

NiO is known under two allotropic varieties: a cubic one and a rhombohedral one. The bunsenite is a green oxide crystallized in a rock-salt structure whose space group is fm3m [23]. Nevertheless, this cubic structure is known to be distorted to a rhombohedral cell whose space group is R-3m [24].

$LiNiO_2$, crystallized in a rhombohedral structure, is a layered compound into which lithium can be deintercalated and re-intercalated [25]. Lithium ions are situated in (3a) sites, nickel ions in (3b) sites and oxygen ions in (6c) sites. When no crystal defect is present in the lattice, $LiNiO_2$ can be described as a succession of three kinds of plan, one containing only lithium, one only oxygen, and a third one only nickel. The prepared compounds are not stoichiometric and the position of lithium as a function of its amount is investigated further on.

4. Results and discussion

4.1. Determination of the lattice parameters of $Li_xNi_{1-x}O$ ($0 < x < 0.5$)

All the synthesized samples including $Li_xNi_{1-x}O$ powders and $Li_xNi_{1-x}O$/Au were analyzed by XRD before exposure to the carbonate melt. Precise lattice parameters and the real lithium content of these compounds were deduced from Rietveld refinement of $Li_xNi_{1-x}O$

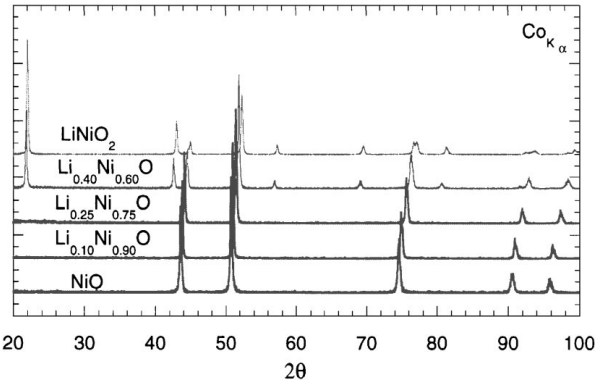

Figure 1 XRD patterns of $Li_xNi_{1-x}O$ ($0 < x < 0.5$) synthesized by soft chemistry route.

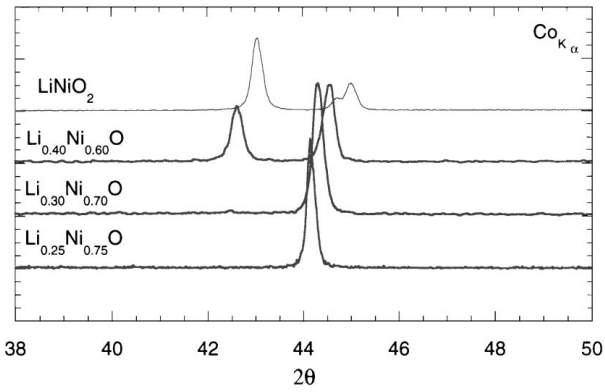

Figure 2 Partial XRD patterns of $Li_xNi_{1-x}O$ with different lithium contents showing the phase change between NiO and $LiNiO_2$ structures.

powders avoiding the interference of gold XRD lines in $Li_xNi_{1-x}O$/Au. In this first case, the precision of the Rietveld method is much better. The XRD patterns of $Li_xNi_{1-x}O$ powders as a function of x are shown in Fig. 1. All the compounds were single-phase, neither other secondary product nor reactant were detected. A phase change can be noted between $x = 0.3$ and $x = 0.4$. Hence, the general feature of NiO structure is conserved for $0 < x < 0.3$ and the general feature of $LiNiO_2$ structure is observed for $0.3 < x < 0.5$.

For $x = 0$, NiO has a rock-salt structure with $a = 4.177$ Å [26]. For $0 < x < 0.3$, $Li_xNi_{1-x}O$ is also cubic and the pattern can be indexed in the Bragg peaks of NiO. There is no preferential position for lithium and nickel ions; thus, there is only one cation crystallographic site. When the amount of lithium increases, the whole pattern is shifted towards larger angles. The partial substitution of nickel (II) ($r = 0.83$ Å) by lithium (I) ($r = 0.90$ Å) implies the creation of nickel (III) ($r = 0.70$ Å) whose ionic radius r is smaller, which contracts the lattice [27]. On the XRD pattern of the $Li_{0.3}Ni_{0.7}O$ compound, a large and very low intensity peak appears around $2\theta = 21^\circ$, which indicates a short-range order of lithium. Moreover, the broadening of (111), (220), (311) and (222) peaks is observed for this compound. This phenomenon becomes more pronounced for the higher lithium content compounds, where all the mentioned lines are split into two. In Fig. 2, the evolution of the XRD pattern, between $x = 0.30$ and $x = 0.50$, is presented. For $x = 0.4$, the (101) line appears and for $x = 0.5$ the splitting of the line $2\theta = 44.5^\circ$ into (006) and (012) can be noted. The significant evolution of the XRD pattern is correlated with the phase transition. Indeed, for $0.3 < x < 0.5$, $Li_xNi_{1-x}O$ is crystallized in a hexagonal system; lithium and nickel ions being segregated into predominant lithium site plan and nickel one. The pattern is close to that of $LiNiO_2$ whose space group is R-3m.

In order to follow the influence of the lithium amount on the lattice parameters, all the compounds were indexed in a hexagonal system. For the compounds with $0 < x < 0.3$, the cubic cell is equivalent to a hexagonal one. Indeed, as mentioned by Li *et al.*, when in a hexagonal cell, $c_h/a_h = 2\sqrt{6}$, it is equivalent to the cubic one with $a_c = \sqrt{2}a_h$ [15]. The evolution of the $\langle\langle a \rangle\rangle$ and $\langle\langle c \rangle\rangle$ parameters is presented in Fig. 3. Both of

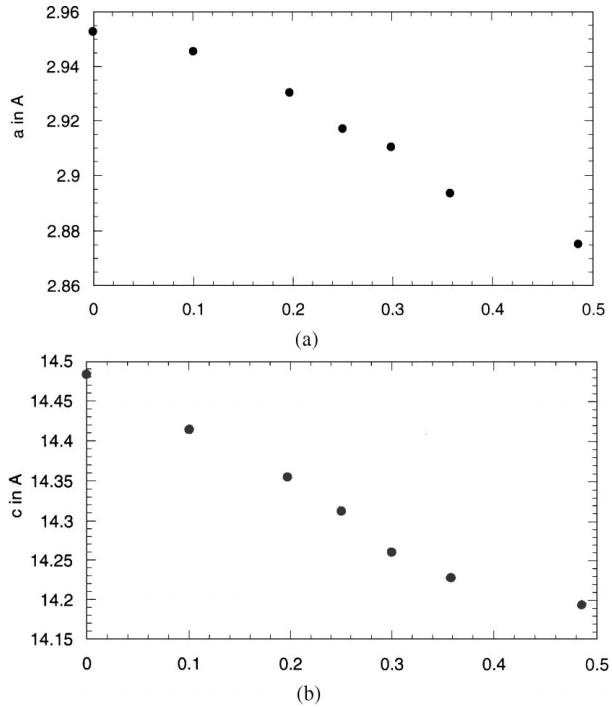

Figure 3 Evolution of the hexagonal parameters of $Li_xNi_{1-x}O$. (a) "a" parameter; (b) "c" parameter.

them decrease progressively, which can be explained by the contraction of the lattice due to the increase in the Ni(III) content as mentioned previously. These results are in agreement with those of Li *et al.* who used a solid state synthesis route [15].

These parameters and the real amount of lithium were deduced from the Rietveld refinement. The final convergence factors varied a little with the sample, depending if the powder was analyzed alone or if it was coated on gold. Convergence parameters were the following R-values, with R_B the Bragg factor: $0.010 < R_B < 0.020$, and R_F the R factor: $0.006 < R_F < 0.015$. The error on these values was inferior to 2%, which can be considered as satisfactory. Nevertheless, the corresponding values for profile R_P and weight-profile R_{WP} are much higher: $0.08 < R_P < 0.176$ and $0.11 < R_{WP} < 0.246$. These poor results can be explained by the inappropriate evaluation of the background in relation with the experimental XRD procedure.

A description of Rietveld refinement and *R* factors is given in the Appendix. In this paper, the stability of $Li_xNi_{1-x}O$ ($0 < x < 0.5$) compounds was studied in the carbonate melt. A priori four phenomena may occur:

– Lithium originated from the melt can be incorporated in the nickel oxide. The amount of lithium may then increase with the time.

– Lithium present in the $Li_xNi_{1-x}O$ compound can diffuse in the melt, which means that the compound is not stable in this melt. This diffusion involves a decrease in the lithium amount.

– The melt has no influence on the amount of lithium in the nickel oxide, which means that each $Li_xNi_{1-x}O$ compound, for $0 < x < 0.5$, is stable in the melt; however, this situation is unlikely.

– $Li_xNi_{1-x}O$ compound is totally transformed into NiO and $LiNiO_2$ [14].

4.2. Behavior of $Li_xNi_{1-x}O$/Au ($0 < x < 0.5$) in Li_2CO_3/Na_2CO_3 at 650°C

These samples were analyzed by XRD after a 48-hours immersion in the melt. Before realizing the analysis, the carbonate layer was removed from the electrode as indicated in the experimental part. XRD pattern of the lithiated nickel oxide formed after exposure to the melt was compared with that of the oxide initially present on gold. All the $Li_xNi_{1-x}O$/Au samples were analyzed. The X-ray diffraction patterns of the $Li_{0.4}Ni_{0.6}O$/Au compounds, before and after the exposure to the melt, are compared in Fig. 4. It can be noted that the structure of $Li_{0.4}Ni_{0.6}O$ is not stable in the melt. Indeed, after the immersion, the detected oxide has a composition close to that of NiO as shown in Fig. 4. The (003) line of $Li_{0.4}Ni_{0.6}O$ disappears. This line is very sensitive to the lithium amount and its arrangement in the lattice; its disappearance confirms that under an air/CO_2 (70-30) atmosphere, high lithium compounds are not stable. The lithium content in the oxide decreases significantly, proving the diffusion of lithium ions towards the bulk of the melt and the transformation of Ni(III) into Ni(II). Hence, in our working conditions, the stable nickel oxide in the melt incorporates very few lithium amounts. However, it can be noted that the lines of gold and those of $LiNiO_2$ are very close, which can mask the detection of $LiNiO_2$. In two recent works, $LiNiO_2$ has been detected after immersion in a carbonate melt [14, 28]. In particular, Iinou *et al.* found that this compound was formed at temperatures higher than 800°C, under a pure oxygen atmosphere; nevertheless, under CO_2-rich atmosphere, lithium content in NiO was very low [28].

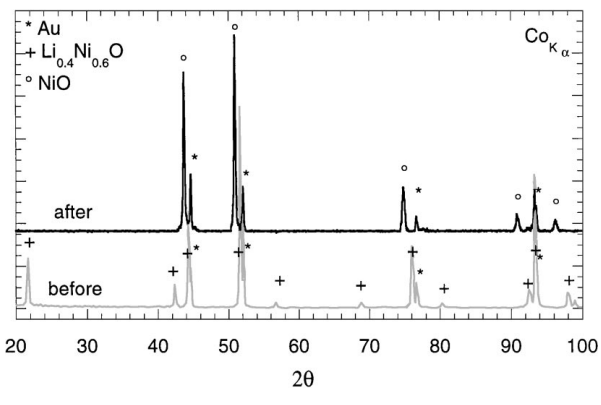

Figure 4 XRD patterns of $Li_{0.4}Ni_{0.6}O$/Au, before and after a 48 h exposure to Li_2CO_3/Na_2CO_3 at 650°C, under air + CO_2, 70-30.

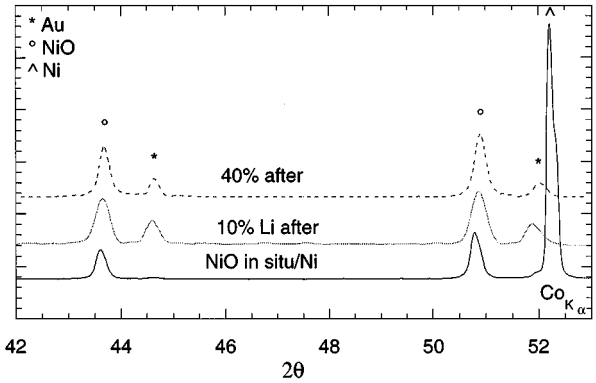

Figure 5 XRD patterns of NiO formed *in situ* on Ni as well as $Li_{0.1}Ni_{0.9}O$/Au and $Li_{0.4}Ni_{0.6}O$/Au after a 48 h exposure to Li_2CO_3/Na_2CO_3 at 650°C, under air + CO_2, 70-30.

All the synthesized samples, analyzed after their immersion, have very close XRD patterns. Whatever the initial oxide, poor or rich in lithium, the nickel oxide after immersion is roughly similar. Hence, the XRD patterns of $Li_{0.1}Ni_{0.9}O$/Au and $Li_{0.4}Ni_{0.6}O$/Au, after exposure to the melt, were compared in Fig. 5 to that of NiO formed *in situ* from metallic nickel. An enlargement of the pattern shows that the product after immersion has a composition rather close to that of NiO formed *in situ* on nickel. However, $Li_{0.1}Ni_{0.9}O$/Au and $Li_{0.4}Ni_{0.6}O$/Au compounds after exposure to the melt, show lines slightly shifted towards larger angles with respect to those relative to the NiO formed *in situ*. This means that lithium content in the mentioned compounds, after exposure to the melt, is a bit higher than in NiO formed *in situ*. The value is close to that 5%. All these results outline the very high stability of nickel oxide, which only incorporates small lithium amounts.

4.3. Estimation of alkali cation content in NiO formed *in situ* on nickel

The amount of lithium in NiO cannot be determined precisely by the Rietveld refinement. Indeed, this content is too weak and the structure factor of lithium is too low. However, an estimation of this content can be obtained. In effect, as shown in Figs 1 and 2, the increase in the lithium content in nickel oxide leads to the shift of the whole XRD pattern towards larger angles. XRD patterns of NiO obtained *in situ* from metallic nickel, of commercial NiO as well as of $Li_{0.05}Ni_{0.95}O$ and $Li_{0.10}Ni_{0.90}O$ prepared *ex situ* are compared before their exposure to the melt in Fig. 6. It can be noted that the (111) line is about $2\theta = 43.5°$ for NiO *in situ*, whereas it is respectively of 43.5°, 43.6°, 43.8° for NiO, $Li_{0.05}Ni_{0.95}O$ and $Li_{0.10}Ni_{0.90}O$. This indicates that the nickel oxide chemically formed *in situ* incorporates much less than 5% of lithium. Furthermore, the

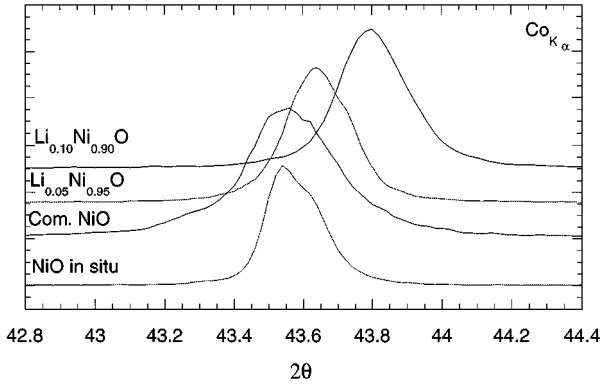

Figure 6 Evolution of the (111) Bragg peak relative to NiO formed *in situ* on Ni, commercial NiO, $Li_{0.05}Ni_{0.95}O$ and $Li_{0.1}Ni_{0.9}O$ synthesized *ex situ*.

XRD pattern of this nickel oxide is very close to that of commercial NiO.

Few amounts of sodium can also be present in the NiO lattice [12]. For the same reasons than lithium, a precise quantification from XRD measurements is impossible. Moreover, contrary to lithium that presents an ideal solid solution, $Li_xNi_{1-x}O$, between NiO and $LiNiO_2$, there is probably no solid solution between NiO and $NaNiO_2$. For example, the synthesis of $Na_{0.2}Ni_{0.8}O$ in the same mentioned conditions was not successful and the final product after thermal treatment was biphased, containing NiO and $NaNiO_2$. Therefore, contrary to lithiated nickel oxide compounds, the study of lattice parameters was not possible for sodium compounds.

The amounts of lithium and sodium in the nickel oxide, after being exposed to the carbonate melt, are very low and analysis techniques such as XPS or XRD are not sensitive enough with respect to light elements. More sensitive techniques as Secondary Ions Mass Spectrometry (SIMS) could be used to evaluate the concentration of lithium in NiO.

Highly lithiated nickel oxides cannot be regarded as alternative cathodes for MCFC because of their high instability. On the contrary, the poorly lithiated nickel oxides synthesized *ex situ* by a soft chemistry process could be valuable. Fluctuations of the lithium ratio between 0–5% may have an important effect on the cathode conductivity. Indeed, an optimization of the lithium content could improve lithiated nickel oxide performances. Moreover, the porous microstructure of the oxide obtained by the precipitate synthesis method might have an interesting electrocatalytic property.

5. Conclusion

Solid solutions of $Li_xNi_{1-x}O$ ($0 < x < 0.5$), in a powder form or deposited on gold, were successfully synthesized by a soft chemistry route. These single-phase compounds were analyzed by XRD before and after their exposure to the molten Li_2CO_3-Na_2CO_3 eutectic. The XRD patterns of $Li_xNi_{1-x}O$ compounds vary between the features of NiO ($0 < x < 0.3$) and $LiNiO_2$ ($0.3 < x < 0.5$) structures. The evolution of cell parameters relative to the synthesized oxides with the increase in the lithium content was followed by the means of Rietveld refinement. A contraction of the lattice was observed with increasing values of x.

$Li_xNi_{1-x}O$ compounds with high lithium content are not stable in the Li_2CO_3-Na_2CO_3 eutectic; lithium ions rapidly diffuse in the melt. It was shown that the lithium content in $Li_xNi_{1-x}O$ compounds, after a 48 h immersion in the melt, reaches a value relatively close to 5%, whereas that obtained with *in situ* formed nickel oxide is significantly lower than 5%. Other more sensitive techniques such as SIMS are required in order to evaluate more precisely the lithium and also the sodium contents in the NiO lattice. The synthesis by a soft chemistry route of $Li_xNi_{1-x}O$ compounds with $x < 5\%$ appears as a new and interesting fabrication procedure for MCFC cathode.

Appendix [29]

The Rietveld algorithm fits the observed diffraction pattern using as variables the instrumental characteristics and the structural parameters of the sample material (lattice and atomic parameters).

The refinement fit minimizes the following function:

$$F = \sum_i w_i (y_{i,\mathrm{obs}} - y_{i,\mathrm{cal}})^2$$

where w_i is the weight assigned to the individual step intensity $y_{i,\mathrm{obs}}$; $y_{i,\mathrm{obs}}$ and $y_{i,\mathrm{cal}}$ are respectively the observed intensity and the calculated intensity at the ith step of the pattern.

The intensity at the ith step is calculated with the following formula:

$$y_{i,\mathrm{obs}} = y_{\mathrm{B},i} + \sum_{hkl} y_{hkl,i}$$

where $y_{B,i}$ is the background intensity at the ith step and $y_{hkl,i}$ is the contribution of each hkl line at the ith step.

Background intensity can be estimated either by a linear interpolation between the points where no peaks appear or by a polynom. Several residual measurements have been introduced to estimate the agreement between the observation and the model. The most useful parameters are the profile and the weighted profile R factors, which take into account the background:

$$R_{\mathrm{p}} = \frac{\sum_i |y_{i,\mathrm{obs}} - y_{i,\mathrm{cal}}|}{\sum_i |y_{i,\mathrm{obs}}|}$$

$$R_{\mathrm{wp}} = \left[\frac{\sum_i w_i (y_{i,\mathrm{obs}} - y_{i,\mathrm{cal}})^2}{\sum_i w_i y_{i,\mathrm{obs}}^2} \right]^{1/2}$$

Two other important factors only take into account the intensity of the integrated lines.

$$R_{\mathrm{Bragg}} = \frac{\sum_{hkl} |I_{hkl,\mathrm{obs}} - I_{hkl,\mathrm{cal}}|}{\sum_{hkl} I_{hkl,\mathrm{obs}}}$$

$$R_{\mathrm{F}} = \frac{\sum_{hkl} |I_{hkl,\mathrm{obs}}^{1/2} - I_{hkl,\mathrm{cal}}^{1/2}|}{\sum_{hkl} I_{hkl,\mathrm{obs}}^{1/2}}$$

where $I_{hkl,\mathrm{obs}}$ is the observed integrated intensity of the (hkl) reflection and $I_{hkl,\mathrm{cal}}$ is the calculated intensity. The R_{Bragg} is surely the best criterion to assess the agreement between the observed data and the structural model.

Acknowledgements

The New Energy and Industrial Technology Development Organization (NEDO) in Japan is acknowledged for financial support. Professor Noël Baffier and Dr Andrée Kahn-Harari are gratefully thanked for their valuable comments and discussions.

References

1. P. H. EICHELBERGER, *J. Power Sources* **171**(1/2) (1998) 95.
2. H. YASUE, H. KATO and K. TAKASU, *ibid.* **171**(1/2) (1998) 89.
3. Y. MUGIKURA, F. YOSHIBA, Y. IZAKI, T. WATANABE, K. TAKAHASHI, S. TAKASHIMA and T. KAHARA, *ibid.* **75** (1998) 108.
4. G. XIE, Y. SAKAMURA, K. EMA and Y. ITO, *ibid.* **32** (1990) 135.
5. P. TOMCZYK, H. SATO, K. YAMADA, T. NISHINA and I. UCHIDA, *J. Electroanal. Chem.* **391** (1995) 125.
6. B. MALINOWSKA, M. CASSIR and J. DEVYNCK, *ibid.* **417** (1996) 135.
7. P. TOMCZYK, H. SATO, K. YAMADA, T. NISHINA and I. UCHIDA, *ibid.* **391** (1995) 133.
8. C. LAGERGREN, A. LUNDBLAD and B. BERGMAN, *J. Electrochem. Soc.* **141**(11) (1994) 2959.
9. G. CHIODELLI, in Fuel Cell Seminar, San Diego, CA, 1994, p. 176.
10. P. PASCAL, "Nouveau Traité de Chimie Minérale," 17th ed. (Masson & C^{ie}, 1963) p. 731.
11. J. R. SELMAN and L. G. MARIANOWSI, in "Molten Salt Technology," edited by D. G. Lovering (Plenum Press, New York, 1982), p. 383.
12. B. MALINOWSKA, M. CASSIR and J. DEVYNCK, *J. Power Sources* **63** (1996) 27.
13. T. NISHINA, K. TAKIZAWA and I. UCHIDA, *J. Electroanal. Chem.* **263** (1989) 87.
14. P. TOMCZYK, J. WYRW and M. MOSIALEK, *ibid.* **463** (1999) 78.
15. W. LI, J. N. REIMERS and J. R. DAHN, *Phys. Rev. B.* **46**(6) (1992) 3236.
16. E. ANTOLINI, *Mat. Chem. Phys.* **52** (1998) 152.
17. D. CAURANT, J. P. PEREIRA-RAMOS, B. GARCIA and N. BAFFIER, *Solid State Ionics* **91** (1996) 45.
18. J. RODRIGUEZ-CARVAJAL, in Collected Abstract of Powder Diffraction Meeting, Toulouse, France, 1990, p. 127.
19. R. W. G. WYCKOFF, "Crystal Structures, Vol 1," 2nd ed. (1963) p. 85.
20. R. W. G. WYCKOFF, "Crystal Structures, Vol 2," 2nd ed. (1964) p. 293.
21. P. VILLARS and L. D. CALVERT, "Pearson's Handbook of Crystallographic Data for Intermetallic Phases, Vol. 2," edited by American Society for Metals (1985) p. 1190.
22. T. SWANSON, *Natl. Bur. Stand.* (U.S.), 539, I, 1953, p. 33.
23. *Idem.*, *Natl. Bur. Stand.* (U.S.), Circ. 539, I, 1953, p. 47.
24. S. WIES and W. EYSEL, Mineral.-Petrograph., Institut des Universitaet Heidelberg, Germany, ICDD Grant-in-Aid (1992).
25. DYER ET AL., *J. Am. Chem. Soc.* **76** (1954) 1499.
26. T. SWANSON, *Natl. Bur. Stand.* (U.S.), 539, I, 1953, p. 47.
27. R. D. SHANNON, *Acta Cryst.* **A32** (1976) 751.
28. S. IINOU, N. MOTOHIRA, N. KAMIYA and K-I. OTA, *Bull. Chem. Soc. Jpn.* **72** (1999) 321.
29. INSTITUT DES MATERIAUX DE NANTES, "Techniques of Analysis of Powder Diffraction (X-ray and Neutrons)" (1991) p. 14.

Received 29 July
and accepted 10 December 1999